

# FIRST PRINCIPLES MATHEMATICAL MODEL AND CONTROL OF A SOLAR THERMAL POWER PLANT

Alice F. Branco<sup>1</sup>, Gustavo A. Andrade<sup>1</sup> and Julio Elias Normey-Rico<sup>1</sup>

<sup>1</sup> Universidade Federal de Santa Catarina, Florianópolis (Brazil)

## Abstract

This paper presents the full mathematical model based on first principle equations of a solar thermal power plant, including a solar collector field, an accumulation tank, and a power conversion system based on the Rankine cycle. The model allows representing the several operational conditions, using or not the energy buffers or auxiliary backup energy source. The inclusion or exclusion of these auxiliary elements during the plant operation produces changes in the system dynamics, which complicates the analysis and modelling of the process. In this work, adequate tools to analyse and predict system behaviour are used. Simulation results are presented to show how the proposed model is able to simulate the configuration modes of the solar system, being useful for both analysis and control design purposes.

*Keywords: Renewable energy, Modelling, Solar thermal power plant.*

---

## 1. Introduction

Currently there is a worldwide effort for sustainable development, due to the combined effects of fossil fuel consumption, limitations in available sources, and the environmental awareness of anthropogenic carbon dioxide emissions impact (Pasamontes et al., 2013). These factors constitute an important driving force behind the introduction of clean and viable alternatives in all energy consuming sectors (Camacho et al., 2012). Among all renewable energy sources, solar energy is being considered as the most promising source of energy.

Thermosolar plants can generate solar power by using mirrors or lenses to concentrate a large area of sunlight onto a small area (Powell and Edgan, 2012). Electricity is generated when the concentrated light is converted to heat, which drives a heat engine connected to an electrical power generator. In this case, these systems are generally composed of a solar collector field, storage tanks, a steam generator, a turbine and a condenser. In order to operate these systems efficiently obtaining the maximum allowable energy, several variables must be controlled in their optimal values. However, thermosolar plants have complex dynamics, containing strong nonlinearities, transport delays and uncertainties, which makes the control design a challenging task (Camacho et al., 2012).

From a control point of view, some efforts have been devoted to controlling the outlet temperature of the solar collector field, such as in Elias (2018), where a hybrid model of the solar collector was used to control the focus of solar field mirrors and optimize the outlet temperature of the solar field in order to obtain safe and cost-effective plant operation conditions. The outlet temperature of a thermal storage system is controlled by using a feedforward internal model controller as shown in Mawire and McPherson (2008). In Kalita (2014) PID, fuzzy logic and neural network predictive controllers were applied to control the drum boiler's water height on a steam generator for comparison.

Depending on the control complexity, different types of system models are required. These models can range from the simplest ones, based on steady-state relationships or on linear low-order approaches to those based on nonlinear first principles (Camacho et al., 2007). The last ones are addressed to advanced control strategies, where an appropriate optimization of the whole system is performed in an upper layer. In addition, a dynamic nonlinear first principles-based model of the system allows determination of experimental values for characteristic thermodynamic properties. However, these models are difficult to obtain due to the necessity of previous knowledge about the system.

In this work, the nonlinear mathematical model and local control structure of a solar thermal power plant is proposed. The solar plant studied in this work is composed of: a solar collector field, one storage tank, a steam generator, a steam turbine and a condenser, which are the most common components for industrial solar thermal power plants. The plant model presented in this work allows to predict the dynamic behaviour of the most important variables (temperature, pressure and volumetric flow) in the different operation modes. In addition, the model can be applied with other purposes, for example, at the plant design stage, the model makes possible to apply a parameter



### 2.1. Solar Collectors Field

The solar collector's field is the main source of energy to the clean energy generator process. It is used to raise the fluid's temperature, in this case oil, to supply the system's heat demand. Each collector panel absorbs heat in the form of solar radiation when it reaches the external surface of the collector, transferring the heat to the molten salt which is flowing inside the pipes in the collector (Powell and Edgar, 2012). The metal that constitutes the pipe goes through a treatment at its surface so it has high absorbing and low emission properties, to absorb high quantities of radiation while minimizing radiating heat loss (Kalogirou, 2013).

The modelling of this subsystem is obtained by calculating the energy balances of the fluid and the metal, assuming that the dominant course of heat transfer is the metal to fluid conduction. Thus, the collector was modelled by two coupled equations, based on the model presented in Camacho et al. (2012) and Álvarez et al. (2007).

The following assumptions were considered for the modelling of the solar collector field (Pasamontes et al., 2013): the fluid is incompressible, its heat capacity is constant; the effects of the pressure gradient fluctuations in the temperature of the thermal molten salt are neglected, and; the pipe's wall heat resistance is dropped out from consideration.

Equation (1) models the metal's temperature dynamic and Equation (2) models the fluid's temperature.

$$\rho_m C_m A_{sc,o} \frac{\partial T_{sc,m}(t)}{\partial t} = d_o \pi \eta I(t) - d_o \pi h_o (T_{sc,m}(t) - T_a(t)) - d_i \pi h_i (T_{sc,m}(t) - T_{sc,f}(t)), \quad (\text{eq. 1})$$

$$\rho_f C_f A_{sc,i} \frac{\partial T_{sc,f}(t,x)}{\partial t} = -\dot{q}_{sc}(t) \rho_f C_f \frac{\partial T_{sc,f}(t,x)}{\partial x} + d_i \pi h_i (T_{sc,m}(t) - T_{sc,f}(t)), \quad (\text{eq. 2})$$

where  $T_{sc,m}$  is the collector's temperature,  $\dot{q}_{sc}$  is the fluid volumetric flow, which will be used as the manipulated variable for the control algorithm,  $I$  is the solar irradiance, a disturbance,  $T_a$  is the ambient temperature, also a disturbance, and  $T_{sc,f}$  is the fluid temperature, which comes from the cold storage tank.

### 2.2. Storage Tank

There are two storage tanks (see Figure 1) in a serial configuration, a hot tank and a cold tank. They work as buffers and are used as energy stock as hot fluid when there is not enough irradiation or demand to sustain the energy generation process (Pasamontes et al., 2013). They can be used also to alleviate the outlet solar collectors' effects of temperature and flow variations on the inlet of the energy generation process. Both tanks will have the same modelling, presented next.

The storage tanks' model is based on the stratified model proposed in (Cruickshank, C. A., Harrison, S. J., 2006), where each tank was subdivided into 3 sections and the heat exchange is calculated between each section. The heat transfer fluid will enter the cold tank through its bottom section, and, because it is hotter than the molten salt inside the tank, it will rise and exit the tank through the upper section, entering the hot tank through the bottom and repeating the process.

Each tank can be considered a buffer, so it is possible to model the heat exchange phenomena as first order dynamic between the input and output temperatures, with different settling times. In Equation (4), it is shown the model used for each section of the tank.

$$\rho_f C_f V_{t,i,j} \frac{\partial T_{t,i,j}(t)}{\partial t} = \rho_f C_f A_{t,i,j} v_t(t) T_{f,t,i,j} + U_{a,t,i,j} S A_{t,i,j} (T_a - T_{t,i,j}(t)) + U_{t,i,j-1,j} A_{t,i,j-1,j} (T_{t,i,j-1}(t) - T_{t,i,j}(t)) + U_{t,i,j,j+1} A_{t,i,j,j+1} (T_{t,i,j+1}(t) - T_{t,i,j}(t)), \quad (\text{eq. 4})$$

where the subscripts  $t, i, j$  refer to time, tank and section, respectively,  $T_{t,i,j}$  is the fluid's temperature,  $v_t$  is the fluid's velocity through the tanks, which comes from the fluid's flow rate on the solar collectors field, and  $T_{f,t,i,j}$  is the fluid's input temperature, which comes from the collector field, for the hot tank, and from the hot tank minus a loss of temperature due to heat exchange with the steam generator, when evaluating the cold tank.

### 2.3. Steam Generator

The steam generator process is complex, especially because it deals with a two-phase process. The heat,  $Q$ , comes from the heated molten salt from the tanks and causes the water flow rate  $q_f$ , which comes from the condenser, to boil and turn to steam flow rate  $q_s$ . Gravity causes the saturated steam to rise, which causes circulation inside the

drum of the steam generator. The input heat is calculated as  $Q = \dot{m}\rho_f\Delta T$ , where  $\dot{m}$  is the volumetric flow rate on the output of the hot storage tank and  $\Delta T$  is the difference in temperature between the output of the hot tank and the input of the cold tank.

The system is quite complex, since there is presence of steam below liquid level, which causes the shrink-and-swell phenomenon. Even though the complexity of the system is considerable, its behaviour can be captured by global mass and energy balances for control purposes (Åström and Bell., 1989).

The models used to describe the system's dynamics are of low order thanks to a key property of steam generators: they have a very efficient heat transfer due to boiling and condensation, which means that the energy is released or absorbed rapidly. This implies that different parts of the boiler change temperature in the same way, so all parts of the system, which are in contact with the saturated liquid-steam will be in thermal equilibrium (Åström and Eklund, 1975).

The model obtained has a state space representation, shown in Equations (5) - (8). The deduction of this model can be found in Åström and Bell (1998). The state variables are the drum pressure,  $p$ , total water volume,  $V_{wt}$ , quality at the riser outlet,  $\alpha_r$ , and volume of steam under the liquid level,  $V_{sd}$ .

$$e_{11} \frac{dV_{wt}}{dt} + e_{12} \frac{dp}{dt} = q_f - q_s, \quad (\text{eq. 5})$$

$$e_{21} \frac{dV_{wt}}{dt} + e_{22} \frac{dp}{dt} = Q + q_f h_f - q_s h_s, \quad (\text{eq. 6})$$

$$e_{32} \frac{dp}{dt} + e_{33} \frac{d\alpha_r}{dt} = Q - \alpha_r h_c q_{sc}, \quad (\text{eq. 7})$$

$$e_{42} \frac{dp}{dt} + e_{34} \frac{d\alpha_r}{dt} + e_{44} \frac{dV_{sd}}{dt} = \frac{\rho_s}{T_d} (V_{sd}^0 - V_{sd}) + \frac{h_f - h_w}{h_c} q_f. \quad (\text{eq. 8})$$

#### 2.4. Steam Turbine

The steam turbine model depends vastly on its size and how much power it should generate. For the model presented in this work, the input variables of the turbine model are pressure, temperature and steam mass flow rate, which come from the steam generator, and the output variables calculated through dynamic models are pressure, temperature, steam mass flow rate and the turbine generated power.

The dynamic model of the turbine was divided in several subsystems: dead space, stage groups on the high, HP, and low, LP, pressure sections, moisture separator and reheater and its general scheme can be seen on Figure 2. To diminish the computational effort, the HP and LP stages were fused in groups and its parameters were averaged (Kulkowski et al., 2017), the process variables after the reheater were linearized and the time constants were considered to be independent of the load (Sokolski et al., 2015).

A dynamic model is necessary to study the transient states for a more accurate calculation of the controllers. However, it must also be as simple as possible to avoid extra computational efforts (Kulkowski et al., 2015) while still having a good representation of the process. To control the generated power, which is the main aim of the control system, it is not necessary to have knowledge of all the intermediary variables of the process.

**Control Valve:** The control valve is used as the actuator of the turbine and it regulates the pressure entering the turbine. To calculate the opening of the control valve,  $\alpha_{CV}$ , a first order ordinary differential equation is used, which can be seen on Equation (9).

$$\tau_{CV} \frac{d\alpha_{CV}^0}{dt} + \alpha = k_{CV} \alpha_{CV}^i. \quad (\text{eq. 9})$$

The output pressure of the control valve,  $P_{CV}^{out}$ , and its mass flow rate,  $M_{CV}^{out}$ , output are calculated based on static models shown on Equations (10) and (11), respectively.

$$P_{CV}^{out} = P_{CV}^{nom,out} \frac{\alpha_{CV}^0}{\alpha_{CV}^{nom,0}}, \quad (\text{eq. 10})$$

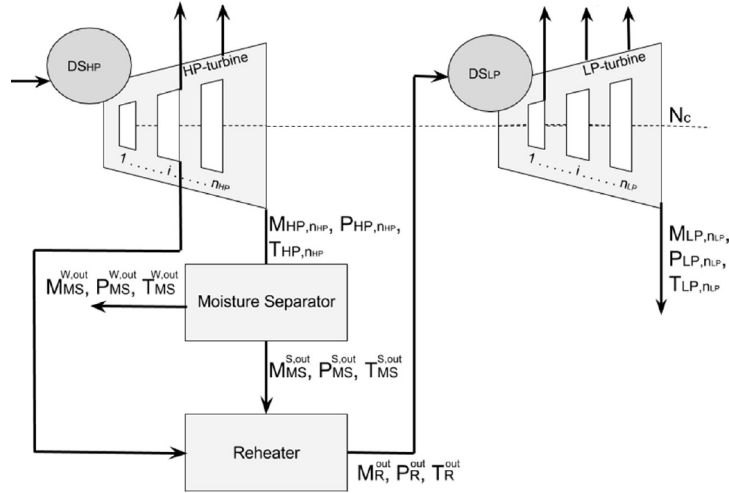


Fig. 2: Schematic of the steam turbine subsystems (Kulkowski et al., 2015)

$$M_{CV}^{out} = M_{CV}^{nom,out} \frac{P}{p^{nom}} \frac{\alpha_{CV}^0}{\alpha_{CV}^{nom,0}}, \quad (\text{eq. 11})$$

where  $\alpha_{CV}^i$  is the reference valve opening degree.

**Dead Space High Pressure Stages:** For the inlet of the HP section, Equations (12) and (13) were used to calculate the outlet pressure dynamic of the dead space,  $P_{DS,HP}^{out}$ . To calculate the outlet mass flow rate and the temperature of the dead space,  $M_{DS,HP}^{out}$  and  $T_{DS,HP}^{out}$ , static relationships were used, seen in Equations (14) and (15), respectively.

$$\tau_{DS,HP} = \frac{V_{DS,HP}}{H_{DS,HP} M_{DS,HP}^{nom,in} \vartheta_{DS,HP}}, \quad (\text{eq. 12})$$

$$\tau_{DS,HP} \frac{dP_{DS,HP}^{out}}{dt} = k_{DS,HP} (M_{DS,HP}^{out} - M_{DS,HP}^{in}), \quad (\text{eq. 13})$$

$$M_{DS,HP}^{out} = M_{CV}^{out}, \quad (\text{eq. 14})$$

$$T_{DS,HP}^{out} = A_{DS} P_{DS,HP}^{out} B_{DS} P_{DS,HP}^{out} C_{DS}. \quad (\text{eq. 15})$$

**High Pressure Stages:** A more complete modelling of the system would involve a dynamic modelling of the high pressure, HP, section. But to diminish the computational effort, a static model of the HP stages was applied, as its dynamic time was considerably low comparing to the other components of the steam turbine. This turbine was considered to have ten stages, represented by  $j$  in the following equations, and two vents after stages three and six. For the calculation of the outlet pressure for each stage,  $P_{HP,j}^{out}$ , Equations (16)- (18) were used. For the calculation of the outlet temperature for each stage,  $T_{HP,j}^{out}$ , Equation (19) was used. For the calculation of the outlet mass flow rate for each stage,  $M_{HP,j}^{out}$ , Equation (20) was used. For each stage with a vent, the calculation of the outlet mass flow rate for each vent,  $M_{HPv,j}^{out}$ , Equation (21) was used.

$$P_{HP,j}^{in} = P_{DS,HP}^{out}, j = 1, \quad (\text{eq. 16})$$

$$P_{HP,j}^{in} = P_{HP,j-1}^{out}, \quad (\text{eq. 17})$$

$$P_{HP,j}^{out} = P_{HP,j}^{nom,out} \frac{P_{HP,j}^{in}}{P_{HP,j}^{nom,in}}, \quad (\text{eq. 18})$$

$$T_{HP,j}^{out} = A_T P_{HP,j}^{out} B_T P_{HP,j}^{out} C_T, \quad (\text{eq. 19})$$

$$M_{HP,j}^{out} = M_{HP,j}^{nom,out} \sqrt{\frac{T_{HP,j}^{nom,in} (P_{HP,j}^{in})^2 - (P_{HP,j}^{out})^2}{T_{HP,j}^{in} (P_{HP,j}^{nom,in})^2 - (P_{HP,j}^{nom,out})^2}}, \quad (\text{eq. 20})$$

$$M_{HPv,j}^{out} = M_{HPv,j}^{nom,out} \frac{M_{HP,j=vent}^{out}}{M_{HP,j=vent}^{nom,out}}, \quad (\text{eq. 21})$$

where  $P_{HP,j}^{in}$ ,  $P_{HP,j-1}^{out}$  are the pressure on the input of each stage and on the output of the stage before, respectively,  $T_{HP,j}^{in}$  is the input temperature on each stage and  $M_{HP,j=vent}^{out}$  is the output mass flow rate of the stage equivalent to the vents' stage.

**Moisture Separator:** The moisture separator separates liquid water from the steam generated, so the pressure, temperature and mass flow rate variables are calculated for the steam, represented by the superscript S on the following equations, and for the liquid water, represented by the superscript W on the following equations. The outlet mass flow rate of the moisture separator,  $M_{MS}^{S,out}$  is calculated by Equations (22) and (23). The water outlet temperature of the moisture separator,  $T_{MS}^{W,out}$  is calculated by Equations (24) and (25). The outlet pressure of the moisture separator,  $P_{MS}^{S,out}$  and  $P_{MS}^{W,out}$  are equal to the outlet pressure of each the output pressure at final stage of the high-pressure section.

$$M_{MS}^{S,in} = M_{HP,j}^{out}, \quad (\text{eq. 22})$$

$$M_{MS}^{S,out} = M_{MS}^{S,in} \frac{x^{in}}{x^{out}}, \quad (\text{eq. 23})$$

$$T_{MS}^{W,in} = T_{HP,j}^{out}, \quad (\text{eq. 24})$$

$$T_{MS}^{W,out} = T_{MS}^{nom,W,out} \left( P_{T3} \frac{T_{MS}^{W,in}}{T_{MS}^{nom,W,in}} + P_{T4} \right), \quad (\text{eq. 25})$$

where  $M_{MS}^{S,in}$  and  $M_{MS}^{W,in}$  are the mass flow rate of the steam on the inlet of the moisture separator and of the water on the inlet of the moisture separator and  $T_{MS}^{W,in}$  is the water temperature on the inlet of the moisture separator.

**Reheater:** To increase the power generated by the turbine, it is necessary to raise the steam temperature, which is done by the reheater. The calculation of the outlet mass flow rate of the reheater,  $M_R^{out}$ , is done accordingly to the Equations (26) and (27). The calculation of the outlet pressure of the reheater,  $P_R^{out}$ , is done accordingly to Equations (28) – (30). The calculation of the outlet temperature of the reheater,  $T_R^{out}$ , is done accordingly to Equation (31).

$$M_R^{in} = M_{MS}^{S,out}, \quad (\text{eq. 26})$$

$$M_R^{out} = M_R^{nom,out} \frac{M_R^{in}}{M_R^{nom,in}}, \quad (\text{eq. 27})$$

$$P_R^{in} = P_{MS}^{S,out}, \quad (\text{eq. 28})$$

$$\tau_R = \frac{V_R}{H_R^{avg} M_R^{nom,out} v_R}, \quad (\text{eq. 29})$$

$$\tau_R \frac{dP_R^{out}}{dt} = k_R (M_R^{in} - M_{LP,1}^{out}), \quad (\text{eq. 30})$$

$$T_R^{out} = T_R^{nom,out} \left( H_T + I_T \frac{P_R^{in}}{P_R^{nom,in}} \right), \quad (\text{eq. 31})$$

where  $M_R^{in}$  and  $M_{LP,1}^{out}$  are the mass flow rate at the input of the reheater and on the outlet of the first group of stages on the LP section, respectively.  $P_R^{in}$  is the pressures on the input of the reheater.

**Dead Space of the Low-Pressure Stages:** For the inlet of the LP section, Equations (32) and (33) were used to calculate the outlet pressure dynamic of the dead space,  $P_{DS,LP}^{out}$ . To calculate the outlet mass flow rate and the temperature of the dead space,  $M_{DS,LP}^{out}$  and  $T_{DS,LP}^{out}$ , static relationships were used, seen on Equations (34) and (35), respectively.

$$\tau_{DS,LP} = \frac{V_{DS,LP}}{H_{DS,LP} M_{DS,LP}^{nom,in} \vartheta_{DS,LP}}, \quad (\text{eq. 32})$$

$$\tau_{DS,LP} \frac{dP_{DS,LP}^{out}}{dt} = k_{DS,LP} (M_{DS,LP}^{out} - M_{DS,LP}^{in}), \quad (\text{eq. 33})$$

$$M_{DS,LP}^{out} = M_R^{out}, \quad (\text{eq. 34})$$

$$T_{DS,LP}^{out} = A_{DS} P_{DS,LP}^{out} B_{DS} P_{DS,LP}^{out} C_{DS}, \quad (\text{eq. 35})$$

Where  $M_{DS,LP}^{in}$  is the mass flow rate on the inlet of the dead space.

**Low Pressure Stages:** The low pressure, LP, section was divided in six stages, with three vents after stages two, four and five. Each stage is represented by  $i$  on the following equations. For the calculation of the outlet pressure for each stage,  $P_{LP,i}^{out}$ , Equations (36) – (38) were used. For the calculation of the outlet temperature for each stage,  $T_{LP,i}^{out}$ , Equation (39) was used. For the calculation of the outlet mass flow rate for each stage,  $M_{LP,i}^{out}$ , Equation (40) was used. For each stage with a vent, the calculation of the outlet mass flow rate for each vent,  $M_{LPv,i}^{out}$ , Equation (41) was used.

$$P_{LP,i}^{in} = P_{DS,LP}^{out}, i = 1, \quad (\text{eq. 36})$$

$$P_{LP,i}^{in} = P_{LP,i-1}^{out}, \quad (\text{eq. 37})$$

$$P_{LP,i}^{out} = P_{LP,i}^{nom,out} \frac{P_{LP,i}^{in}}{P_{LP,i}^{nom,in}}, \quad (\text{eq. 38})$$

$$T_{LP,i}^{out} = A_T P_{LP,i}^{out} B_T P_{LP,i}^{out} C_T, \quad (\text{eq. 39})$$

$$M_{LP,i}^{out} = M_{LP,i}^{nom,out} \sqrt{\frac{T_{LP,i}^{nom,in} (P_{LP,i}^{in})^2 - (P_{LP,i}^{out})^2}{T_{LP,i}^{in} (P_{LP,i}^{nom,in})^2 - (P_{LP,i}^{nom,out})^2}}, \quad (\text{eq. 40})$$

$$M_{LPv,i}^{out} = M_{LPv,i}^{nom,out} \frac{M_{LP,i=vent}^{out}}{M_{LP,i=vent}^{nom,out}}. \quad (\text{eq. 41})$$

where  $P_{LP,i}^{in}$  and  $P_{LP,i-1}^{out}$  are the pressure at the input of each stage and at the output of the each stage, respectively,  $T_{LP,i}^{in}$  is the input temperature of each stage and  $M_{LP,i=vent}^{out}$  is the output mass flow rate of the stage equivalent to the vents' stage.

**Mechanical Power:** Firstly, an enthalpy drop,  $\Delta h^{out}$  is calculated using Equation (42), for each stage group on the HP and LP sections. Then, the theoretical power is calculated on each group of stages,  $N_C$ , according to the calculated enthalpy drop, as shown in equations (43) and (44), where  $T^{in}$  is the temperature on the input of each stage on the HP or LP sections and  $P^{out}$  and  $P^{in}$  are the pressure on the output and the input of each stage on the HP or LP sections, respectively.  $M_{s,k}^{out}$  is the outlet mass flow rate of each stage. The effective power of the turbine,  $N_T$ , is calculated based on the theoretical power calculated, as can be seen in Equations (45) and (46).

$$\Delta h^{out} = \Delta h^{nom,out} \left( \frac{T^{in}}{T^{nom,in}} \frac{1 - \left(\frac{P^{out}}{P^{in}}\right)^{\frac{H-1}{H}}}{1 - \left(\frac{P^{nom,out}}{P^{nom,in}}\right)^{\frac{H-1}{H}}} \right), \quad (\text{eq. 42})$$

$$N_{s,k} = N_{s,k}^{nom} \frac{k_{s,k}^{nom}}{\eta_{s,k}^{nom}} \frac{M_{s,k}^{out}}{M_{s,k}^{nom,out}} \frac{\Delta h_{s,k}^{out}}{\Delta h_{s,k}^{nom,out}}, \quad (\text{eq. 43})$$

$$N_C = \sum_{s \in \{HP, LP\}, i \in \{1, \dots, n_s\}} N_{s,k}, \quad (\text{eq. 44})$$

$$\eta_e = \eta_e^{nom} \left( \frac{N_C}{N_C^{nom}} \right)^{A \eta \left( \frac{N_C}{N_C^{nom}} \right)^2}, \quad (\text{eq. 45})$$

$$N_T = N_C \frac{\eta_e}{\eta_e^{nom}}. \quad (\text{eq. 46})$$

## 2.5. Electrical Power Generator

The power generator is an equipment which generates electric power from mechanical power. Although it can be modelled with many states, depending on the rotation of the motor and many variables, the model used in this work is simplified, since the non-linear dynamics will be modelled directly on the steam turbine.

The modelling of the electrical power generator was simplified to a first order linear model (Zimmermann, 2012). The model's output is the variation of rotational velocity (Menarin, 2013),  $\Delta\omega$ , and it is calculated using Equation (47). The system's main goal is to maintain the angular velocity at its operating point, which is the frequency of the electric grid. In this case, the frequency of the electric grid is 60Hz and the aim is to maintain  $\Delta\omega = 0$ , in other words, maintain the variation of the grid's frequency at a zero.

$$\tau_G \frac{d\Delta\omega}{dt} + \Delta\omega = N_T - N_D, \quad (\text{eq. 47})$$

where  $N_T$  is the power generated by the steam turbine and  $N_D$  is the power demand.

### 2.6. Condenser

The condenser is a part of the thermal equipment that allows two fluids with different temperatures to transfer heat between each other in adjacent chambers (Americano, 2013) so that the hot fluid will change its phase. In this work, it will be used to transfer heat between the steam that exits the turbine and the water at room temperature, so the steam will condensate, turn into water and go through the first heat exchanger again.

The condenser, much like the steam generator, is also a complex system since it is a two-phase system. The high number of parameters and its non-linear dynamics makes its modelling a complex matter. For the purpose of this work, it will be simplified as a static model, since the dynamics of the steam generator and turbine are more relevant for the simulation and control calculation than the dynamics of the condenser. Some assumptions were made to calculate the model: there is no pressure drop in the steam side, no sub cooling occurs and the enthalpy of the steam at the condenser output equals the saturated liquid enthalpy at the condensing pressure (Patnode, 2006).

Firstly, the condenser's effectiveness,  $\varepsilon(t)$ , is calculated using Equation (48), where  $\dot{m}_w(t)$  is the cooling water's flow rate,  $UA(t)$  is the heat transfer conductance-area product and  $NTU(t)$  is the number of transfer units. The water's temperature,  $T_w(t)$ , is calculated using Equation (49), where  $h_{s,out}(t)$  is the output enthalpy of the steam.

$$UA(t) = UA_{ref} \frac{\dot{m}_w(t)^{0.8}}{\dot{m}_{w,ref}},$$

$$NTU(t) = \frac{UA(t)}{\dot{m}_w(t)C_w}, \quad (\text{eq. 48})$$

$$\varepsilon(t) = 1 - e^{-NTU(t)}.$$

$$T_w(t) = \frac{h_{s,out}(t)}{C_w}. \quad (\text{eq. 49})$$

The heat transfer between the water and the steam and its maximum heat transfer possible,  $Q(t)$  and  $Q_{max}(t)$  respectively, are calculated using Equation (50), where  $\dot{m}_s(t)$  is the steam's input flow rate,  $h_{s,in}(t)$  is the input enthalpy of the steam and  $T_{w,in}(t)$  is the cooling water's input temperature.

$$Q(t) = \dot{m}_s(t) (h_{s,in}(t) - h_{s,out}(t)),$$

$$Q_{max}(t) = \dot{m}_w(t)C_w (T_w(t) - T_{w,in}(t)). \quad (\text{eq. 50})$$

The efficiency of the condenser is calculated using Equation (51).

$$\varepsilon(t) = \frac{Q(t)}{Q_{max}(t)}. \quad (\text{eq. 51})$$

Equalling the above Equations (51) and (48), and substituting Equations (49) and (50), the steam's output enthalpy value is found and, with its value and the condense pressure of the steam turbine, the output temperature of the steam is calculated. While simplified, this model is a good representation of the phase change from steam to liquid water. Its output temperature is one of the steam generator's input.

## 3. Results

The models shown above were simulated using Matlab and the function ode45 with relative tolerance of  $10^{-6}$  to solve the differential equations. When the equipment are connected on serial configuration, the previous equipment's output will be the input of the following one. A control structure containing PI and P controllers was added to the system to maintain each equipment as close as possible to its operation point. The tuning for each controller was



done by pole-cancelling or Ziegler-Nichols and the fine tuning was done by empirical method. The main disturbances, solar irradiation and power demand, can be seen in Figures 4 and 6. As the measurements of power demand were only available with 10 min sampling time, and the simulations require the demand to be provided for every 3 seconds, linear interpolation was performed in order to provide inputs at the necessary sampling time. The simulation results for each equipment are shown in Figures 4 to 6.

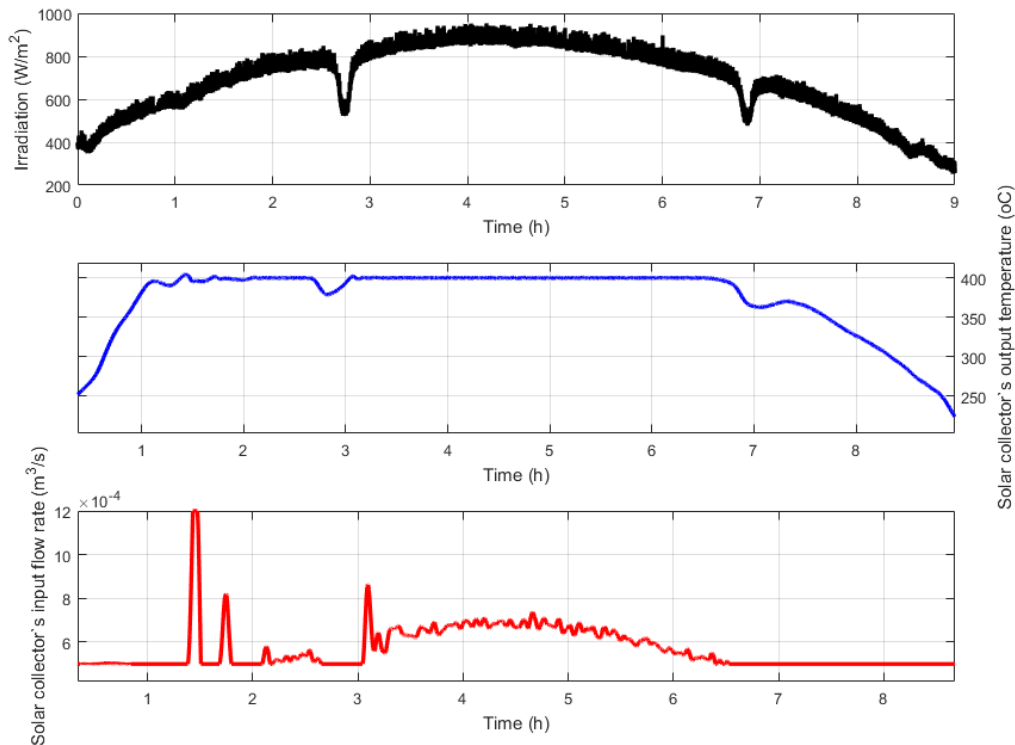


**Fig. 4: Molten salt section behaviour: (a) Solar irradiation, (b) Solar collector's output temperature, (c) Solar collector's output flow rate**

In Figure 4, the system's molten salt section behaviour is shown. The input flow rate in the solar collectors field must be controlled so the hot tank's output temperature is maintained at the desired value for energy generation. The controller calculates the flow rate to raise the collector's output temperature and since it has an inverse gain relationship with the output temperature, the flow rate is kept low, thus the temperature increases at the beginning of the simulation.

The steam generator's and hot storage tank's simulation results can be seen in Figure 5. To raise the storage tanks' output temperature, the flow rate is set to its maximum value so the heated molten salt from the solar field must enter the tank to increase its output temperature. For most of the simulation, both the hot tank's and the collector's output temperature are kept at approximately its operating point, decreasing a few degrees when clouds pass in front of the sun.

The steam generator's dynamic response can be seen in Figure 5. A PI controller is added to regulate its output pressure. The output pressure is controlled through its heat input, which depends on the hot tank's output flow rate. The PI controller applied to control its output pressure by manipulating the hot tank's output flow has a satisfactory result, maintaining the steam generator's pressure at its operating point.

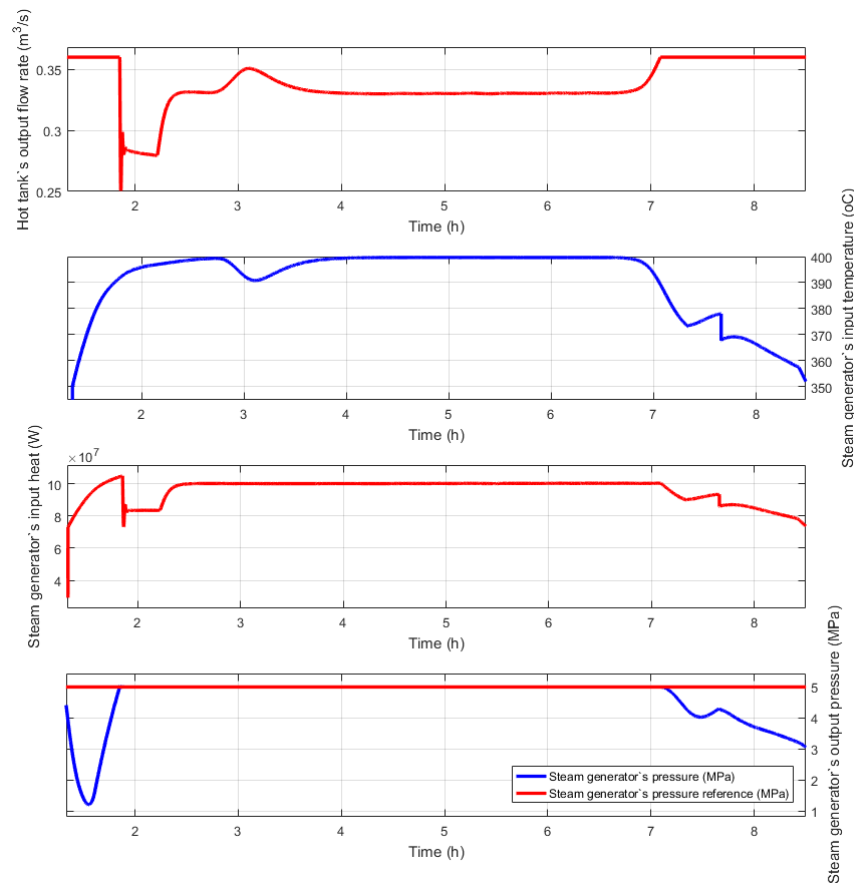


Fig. 5: Steam generator's behaviour: (a) Hot tank's output flow rate, (b) Steam generator's input temperature, (c) Steam generator's input heat, (d) Steam generator's output pressure

A PI controller aims to manipulate the valve opening to generate power by the steam turbine. The maximum power the steam turbine generates is 8 MW, thus, when the power demand is higher, it is not possible to generate the electrical power necessary. The electrical power generator's output, its angular velocity variation, should be zero so that the demand is supplied without energy quality loss. If more pressure is needed, like it occurs at the end of the simulation, the steam turbine's valve is completely opened but the velocity does not track the reference.

With the local controllers maintaining the variables at their respective operating point, the process is capable of generating 8 MW. To increase the power generation when necessary, there would have to be an increase on the turbine's input pressure, that is, in the steam generator's output pressure. However, the pressure is maintained at its reference value, which is its maximum value. It is not ideal to maintain the steam generator's output pressure always at its maximum value, thus advanced controllers can be added to operate on the turbine's valve opening and steam generator's pressure, aiming to produce the necessary power by manipulating both variables.

#### 4. Conclusions

This work presented the modelling of a solar energy plant, through first principle models. Each equipment was modelled separately, and then brought together to simulate the whole process. The energy generation system modelling is done by applying energy, mass and momentum conservation law to each equipment. The main variables calculated on each subsystem are temperature, flow rate and pressure. The previous equipment's output will be the following's input, since connection losses between the subsystems were not considered in this work.

Once defined the separate models, they were brought together and a simulation with real disturbance data was done to analyse the process dynamics and how each equipment influenced the following's response. It is recommended, as a future work, that the modelling done is used to calculate and apply advanced control strategies to generate clean, renewable energy. To guarantee there will be enough energy generated, a gas heater can be added to the modelling, between the steam generator and turbine, to increase the steam's pressure and thus, increase the energy generated.

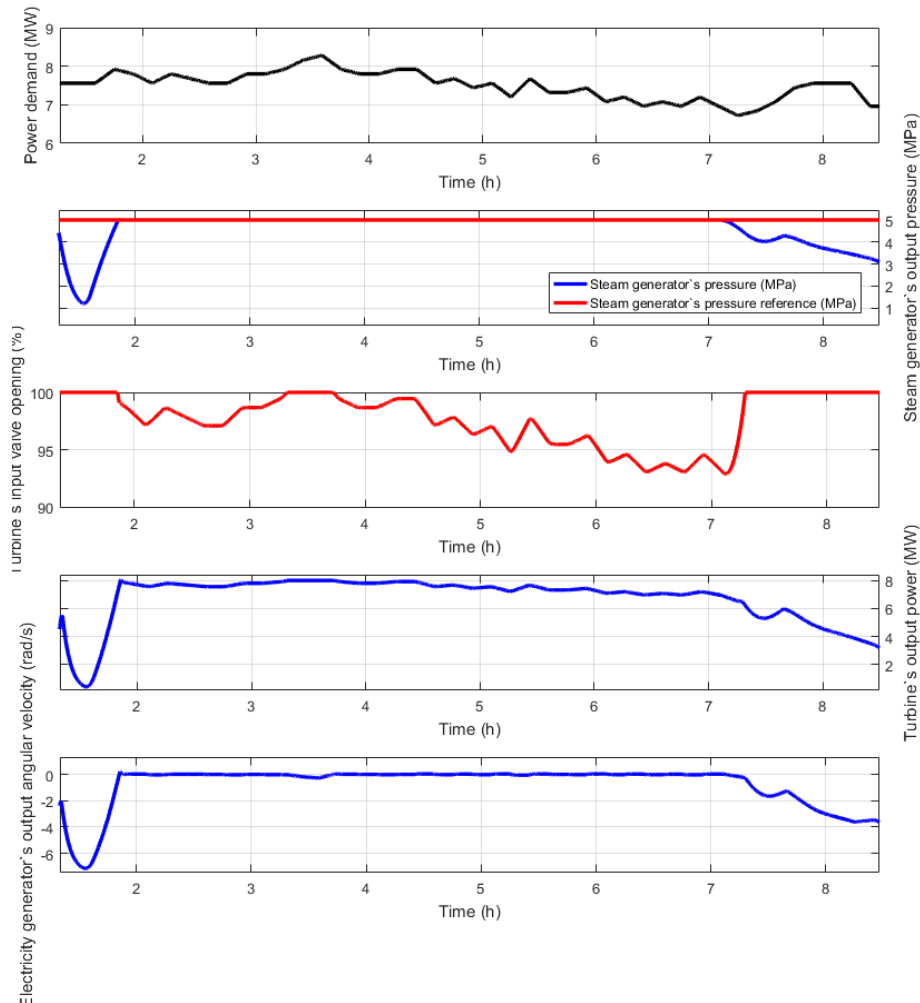


Fig. 6: Power generation section's behaviour: (a) Power demand disturbance, (b) Steam generator's output pressure, (c) Turbine's input valve opening, (d) Turbine's output power, (e) Electrical power generator's output angular velocity

## 5. Acknowledgments

This work has been developed within the context of all activities related to the R&D project registered with ANEEL under the code PD-00553-0042/2016 and sponsored by Petroleo Brasileiro (PETROBRAS).

The authors are thankful for the financial support from Petrobras/ANEEL, R&D project PD-00553-0042/2016 and from CNPq, project 305785/2015-0.

## 6. References

- Álvarez, J. D., Yebra, L. J., Berenguel, M., 2007. Repetitive control of tubular heat exchangers. *Journal of Process Control*. 17, 689 – 701.
- Americano, M. V., 2013. Modelagem, Controle e Otimização de Processos da Indústria do Etanol: uma Aplicação em Energia Solar. Master thesis. Federal University of Santa Catarina, Florianópolis (in Portuguese).
- Anderson, J., 1995. *Computational fluid dynamics: the basics with applications*, first ed. McGraw-Hill series in mechanical engineering.
- Åström, K. J., Eklund, K., 1975. A simple non-linear drum boiler model. *International Journal of Control*. 22, 739-740.
- Åström, K. J., Bell, R. D., 1989. Simple drum-boiler models. *Power Systems: Modelling and Control Applications*. Elsevier. 123-127.
- Åström, K. J., Bell, R. D., 1998. Drum-Boiler Dynamics. *Automatica*. 36, 363 – 378.

- Bonivento, C., Castaldi, P., Mirotta, D., 2001. Predictive control vs PID control of an industrial heat exchanger. 9th Mediterranean Conference on Control and Automation.
- Camacho, E. F., Berenguel, M., Rubio, F. R., Martínez, D., 2012. Control of Solar Energy Systems. IFAC Proceedings Volumes. 45, 848 - 855.
- Camacho, E. F., Rubio, F. R., Berenguel, M., Valenzuela, L., 2007. A survey on control schemes for distributed solar collector fields. Part I: Modelling and basic control approaches. Solar Energy. 81, 1240-1251.
- Cruikshank, C. A., Harrison, S. J., 2006. Experimental Characterization of a Natural Convection Heat Exchanger for Solar Domestic Hot Water Systems. Solar Energy. 425 - 431.
- Elias, T. A., 2018. Hybrid Model Predictive Control for Solar Fields. Master thesis. Federal University of Santa Catarina, Florianópolis.
- Kalita, D., 2014. Modelling, Simulation and Control of a Drum Boiler. Master thesis. Department of Chemical Engineering Birla Institute of Technology and Science, Pilani.
- Kalogirou, S. A., 2013. Solar Energy Engineering: Processes and Systems, second ed. United States: Academic Press.
- Kulkowski, K., Kobylarz, A., Grochowski, M., Duzinkiewicz, K., 2015. Dynamic model of nuclear power plant steam turbine. Archives of Control Sciences. 25.
- Kulkowski, K., Grochowski, M., Duzinkiewicz, K., Kobylarz, A., 2017. Nuclear power plant steam turbine modelling for model-based control purposes. Applied Mathematical Modelling. 48, 491 - 515.
- Mawire, A, McPherson, M., 2008. A feedforward IMC structure for controlling the charging temperature of a TES system of a solar cooker. Energy Conversion and Management. 49, 3143 – 3154.
- Menarin, H. A., 2013. Regulador MPC de Tensão e Velocidade Integrado para Unidades Geradoras Hidrelétricas. Universidade Federal de Santa Catarina (in Portuguese).
- Pasamontes, M., Álvarez, J. D., Guzmán, J. L., Berenguel, M., Camacho, E. F., 2013. Hybrid modelling of a solar-thermal heating facility. Solar Energy. 97, 577 - 590.
- Patnode, A., 2006. Simulation and performance evaluation of parabolic trough solar power plants. Master thesis. University of Wisconsin-Madison, Madison.
- Powell, K. M., Edgar, T. F., 2012. Modeling and control of a solar thermal power plant with thermal energy storage. Chemical Engineering Science. 71, 138-145.
- Sokolski, P., Kulkowski, K., Kobylarz, A., Duzinkiewicz, K., Rutkowski, T. A., Grochowski, M., 2015. Advanced control structures of turbo generator system of nuclear power plant. Acta Energetica.
- Xia, L., Deabreu-Garcia, J. A., Hartley, T. T., 1991. Modelling and simulation of a heat exchanger. Akron University.
- Zimmermann, G. G., 2012. Desenvolvimento de um Controlador MPC para Regulação de Velocidade e Potência Ativa de Turbinas Hidráulicas. End of Course Thesis. Federal University of Santa Catarina (in Portuguese).

## Appendix: Symbols

Table 1: List of symbols

Quantity	Symbol	Unit
Specific heat	$C$	$\text{J kg}^{-1} \text{K}^{-1}$
Diameter	$d$	m
Density	$\rho$	$\text{kg m}^{-3}$
Area	$A$	$\text{m}^2$
Heat transfer coefficient	$h$	$\text{W m}^{-2} \text{K}^{-1}$
Volume	$V$	$\text{m}^3$
Loss coefficient per surface unit	$U$	$\text{W m}^{-2} \text{K}^{-1}$

Table 2: List of symbols

Quantity	Symbol	Unit
Surface area	$SA$	$\text{m}^2$
Time constant	$\tau$	
Gain constant	$k$	
Adiabatic exponent	$H$	
Specific steam volume	$v$	$\text{m}^3 \text{kg}^{-1}$
Temperature coefficients	$A, B, C$	
Steam fraction	$x$	
Efficiency	$\eta$	